Figures and figure supplements

Proteolytic maturation of $\alpha_2\delta$ represents a checkpoint for activation and neuronal trafficking of latent calcium channels
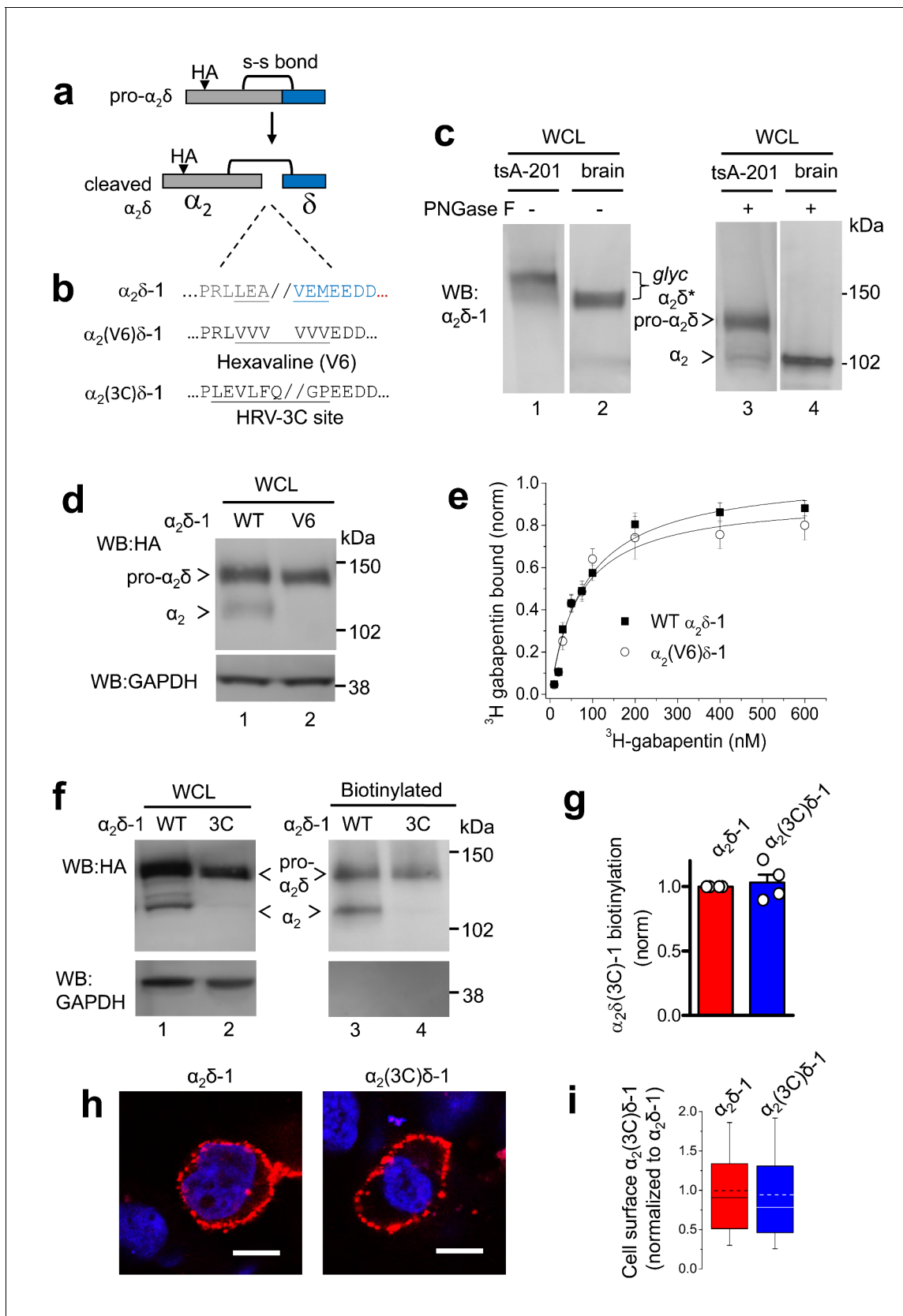
Ivan Kadurin *et al*

Figure 1. Effect of mutation of $\alpha_2\delta$-1 to disrupt the proteolytic cleavage site. (a) Cartoon of uncleaved pro-$\alpha_2\delta$-1 and cleaved $\alpha_2\delta$-1, showing the approximate position of inserted HA tag and disulfide bonds between α_2 (grey) and δ (blue). (b) Rat $\alpha_2\delta$-1 sequence at the identified cleavage-site.
Figure 1 continued on next page

Figure 1 continued

The underlined sequence (including LEA//VEM) in $\alpha_2\delta$-1 was mutated to a V6 or 3C-protease motif. (**c**) Comparison of glycosylated (lanes 1, 2) and deglycosylated $\alpha_2\delta$-1 (lanes 3, 4), expressed in tsA-201 cells (lanes 1, 3) or present in the brain (lanes 2, 4), showing resolution between pro-$\alpha_2\delta$-1 and the cleaved form of $\alpha_2\delta$ after deglycosylation. $\alpha_2\delta^*$ indicates glycosylated species, and pro-$\alpha_2\delta$ and α_2 indicate deglycosylated proteins. Uncleaved pro-$\alpha_2\delta$-1 is observed in transfected cells, but not brain. Proteins visualized with α_2-1 Ab. (**d**) $\alpha_2\delta$-1-HA (left) and α_2(V6)δ-1-HA (right) expressed in tsA-201 cells; proteins deglycosylated with PNGase-F. Upper panel: HA-blots, lower panel: endogenous GAPDH loading control. (**e**) Normalized binding curves, using DRM fractions from transfected tsA-201 cells, for ^{3}H-gabapentin binding to WT $\alpha_2\delta$-1 (■, n = 4) and α_2(V6)δ-1 (○, n = 4). Mean (± SEM) data are fit by hyperbolae with K_D of 82.3 and 68.3 nM, respectively. (**f**) Imunoblot analysis of deglycosylated $\alpha_2\delta$-1-HA and α_2(3C)δ-1-HA. WCL input (lanes 1, 2) and cell-surface biotinylated material (lanes 3, 4) are shown. Upper panel: HA-blot, lower panel: endogenous GAPDH. (**g**) Mean ± SEM (and individual data points) of α_2(3C)δ-1 (blue) cell surface levels, measured as a proportion of biotinylated: total protein, normalized to control (WT $\alpha_2\delta$-1; red), for 4 experiments including that shown in (**f**). p=0.5057, one sample t test. (**h**) Cell-surface expression of $\alpha_2\delta$-1-HA (left) and α_2(3C)δ-1-HA (right) in non-permeabilized tsA-201 cells, using HA Ab (red). Nuclei visualized with DAPI (blue). Scale bars 20 μm. (**i**) Box and whisker plots for quantification of $\alpha_2\delta$-1 on cell-surface, from HA fluorescence, for experiments including (**h**), for WT $\alpha_2\delta$-1 (red) and α_2(3C)δ-1 (blue). N = 290 and 317 cells, respectively, from 3 separate transfections, normalized to WT $\alpha_2\delta$-1 in each experiment. p=0.259, Student's t test.

Accession number	Species	Sequence
NP_001075745	Oryctolagus cuniculus	TFPRLLEA/ADMEDDDFTASMSK
NP_037051.2	Rattus norvegicus	TFPRLLEA VEMEEDDFTASMSK
XP_010976290	Camelus dromedarius	TFPRLLEA VEMEEDDFTASLSK
XP_014710873	Equus asinus	TFPRLLEA VEMEEDDFTASLSK

Figure 1—figure supplement 1. Alignment of the proteolytic cleavage site in $\alpha_2\delta$-1, showing species conservation. / indicates cleavage site previously identified in rabbit $\alpha_2\delta$-1 by N-terminal sequencing of delta *Jay et al., 1991*; *De Jongh et al., 1990*.
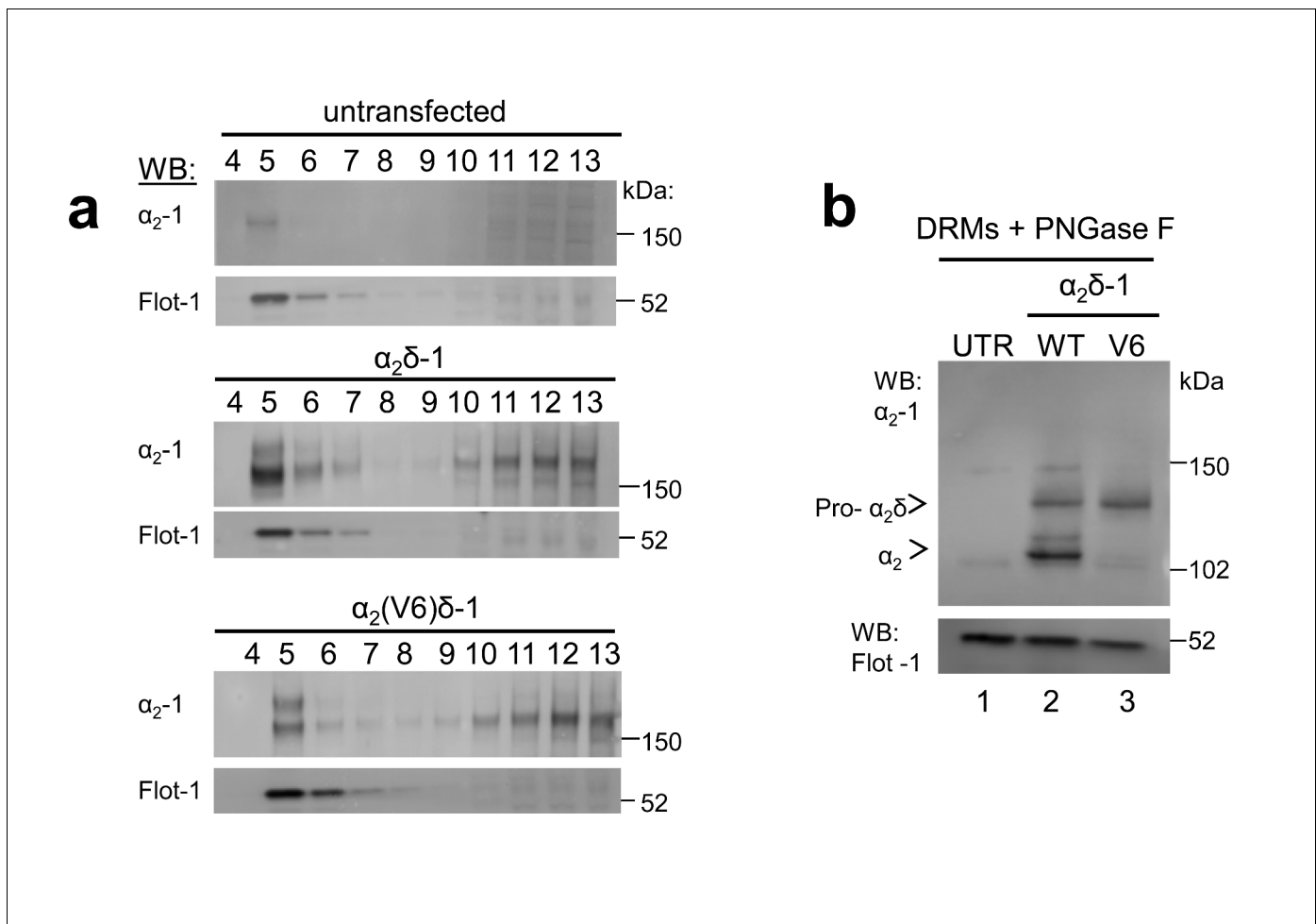
Figure 1—figure supplement 2. α_2(V6)δ-1 is localised in DRMs to a similar extent to $\alpha_2\delta$-1. (a) Sucrose gradient fractions showing a comparison of DRM localisation (lanes 2–4) of $\alpha_2\delta$-1 in untransfected (UTR) tsA-201 cells (top panels, showing some endogenous $\alpha_2\delta$-1), $\alpha_2\delta$-1 transfected cells (middle panels) and α_2(V6)δ-1-transfected cells (bottom panels). The upper panel is a Western blot with $\alpha_2\delta$-1 mAb, and the lower panel of each set shows Flotillin-1 (Flot-1) a DRM marker. (b) Deglycosylation of the peak DRM fractions from the three conditions shown in A, demonstrating the absence of any proteolytic cleavage of α_2(V6)δ-1 (lane 3). The small amount of free α_2-1 indicated is identical to that in the UTR cells (lane 1).
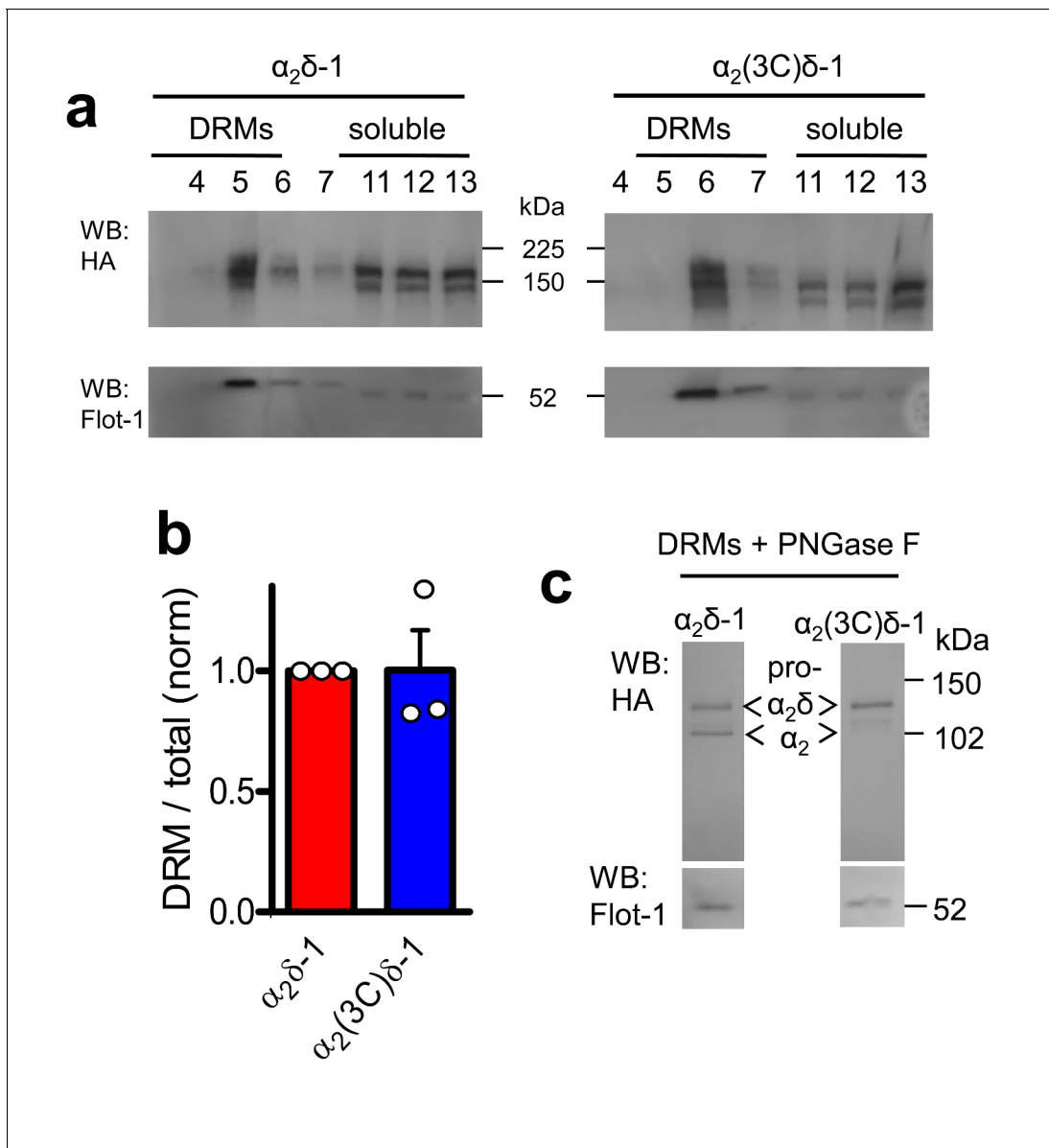DOI: 10.7554/eLife.21143.004

Figure 1—figure supplement 3. $\alpha_2(3C)\delta$-1 is localised in DRMs to a similar extent to $\alpha_2\delta$-1. (a) Comparison of DRM localisation of $\alpha_2\delta$-1-HA (left panels) and $\alpha_2(3C)\delta$-1-HA (right panels), isolated from transfected tsA-201 cells. Only peak DRM (4–7) and soluble (11–13) fractions are shown. The upper panel is a Western blot with HA Ab, and the lower panels show Flotillin-1 (Flot-1), a DRM marker. (b) Quantification of DRM localization for $\alpha_2\delta$-1 (red) and $\alpha_2(3C)\delta$-1 (blue), expressed as DRM/total for n = 3 experiments, normalized to the DRM localization for WT $\alpha_2\delta$-1 in each experiment. Mean ± SEM and individual data points. (c) Deglycosylation of the peak DRM fractions from the two conditions shown in A, demonstrating the absence of any proteolytic cleavage of $\alpha_2(3C)\delta$-1. Flot-1 (lower panel) is a loading control.
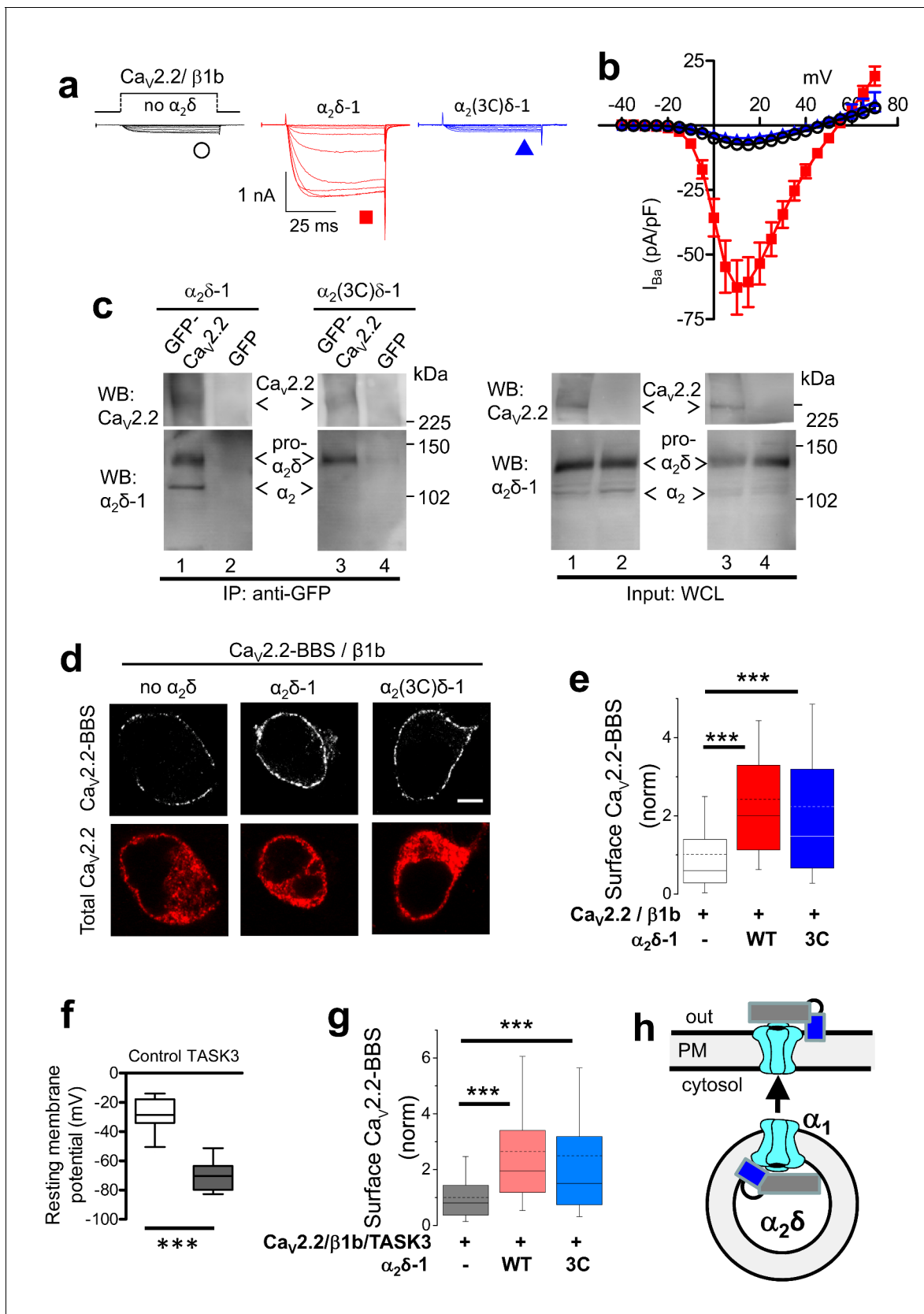DOI: 10.7554/eLife.21143.005

Figure 2. Effect of mutation of $\alpha_2\delta$-1 cleavage site to an HRV-3C site on cell-surface expression and functional properties of Ca$_V$2.2. (a) Example traces (−30 to +10 mV in 5 mV steps) for Ca$_V$2.2/β1b-GFP and no $\alpha_2\delta$ (black traces), WT $\alpha_2\delta$-1 (red traces) or α_2(3C)δ-1 (blue traces). Charge carrier 1 mM

Figure 2 continued on next page

Figure 2 continued

Ba^{2+}. Scale bars refer to all traces. (**b**) Mean (± SEM) *IV* curves for Ca$_V$2.2/β1b-GFP and no α$_2$δ (black open circles, n = 14), WT α$_2$δ-1 (red squares, n = 34) or α$_2$(3C)δ-1 (blue triangles, n = 21). G$_{max}$: 0.25 ± 0.04, 1.91 ± 0.30 and 0.20 ± 0.03 nS/pF, respectively. V$_{50,act}$: 2.85 ± 0.68, 3.33 ± 0.46 and 3.89 ± 0.53 mV, respectively. (**c**) tsA-201 cells transfected with GFP-Ca$_V$2.2 (lanes 1 and 3) or GFP (lanes 2 and 4), plus β1b, and either WT α$_2$δ-1 (lanes 1 and 2) or α$_2$(3C)δ-1 (lanes 3 and 4). Immunoprecipitation of GFP-Ca$_V$2.2 with anti-GFP Ab; WB with Ca$_V$2.2 II-III loop Ab (upper panels, lanes 1 and 3) produced co-immunoprecipitation (lower panels) of WT α$_2$δ-1 (lane 1) and α$_2$(3C)δ-1 (lane 3), revealed by α$_2$δ-1 mAb. Right panels: WCL input for lanes 1–4: upper panels, Ca$_V$2.2-GFP input; lower panels, α$_2$δ-1 input. All samples deglycosylated. (**d**) Immunocytochemical detection of cell-surface expression of Ca$_V$2.2-BBS, with β1b, and empty vector (left), WT α$_2$δ-1-HA (middle) or α$_2$(3C)δ-1-HA (right) in N2A cells. Upper panel: Ca$_V$2.2-BBS cell-surface staining prior to permeabilization (grey-scale); lower panel: total Ca$_V$2.2 after permeabilization (II-III loop Ab, red). Scale bar 5 µm. (**e**) Quantification of Ca$_V$2.2-BBS cell-surface expression (box and whisker plots) with empty vector (open bar, n = 206), WT α$_2$δ-1 (red bar, n = 191) or α$_2$(3C)δ-1 (blue bar, n = 181). Statistical differences: ANOVA and Bonferroni post-hoc test; ***p<0.001, compared to no α$_2$δ. (**f**) Resting membrane potential of control N2A cells (white bar, n = 16) and following expression of TASK3 (gray bar, n = 12). Box and whisker plots; ***p<0.0001, Student's t test. (**g**) Quantification of Ca$_V$2.2-BBS cell-surface expression in N2A cells co-expressing TASK3, with empty vector (gray bar, n = 70), WT α$_2$δ-1 (pink bar, n = 73) or α$_2$(3C)δ-1 (pale blue bar, n = 81). Box and whisker plots, statistical differences: ANOVA and Bonferroni post-hoc test, compared to no α$_2$δ; ***p<0.001. (**h**) Cartoon showing the ability of 'latent' Ca$_V$2.2 (cyan) plus α$_2$(3C)δ-1 (grey α$_2$, blue δ), to traffic to the plasma membrane (PM).
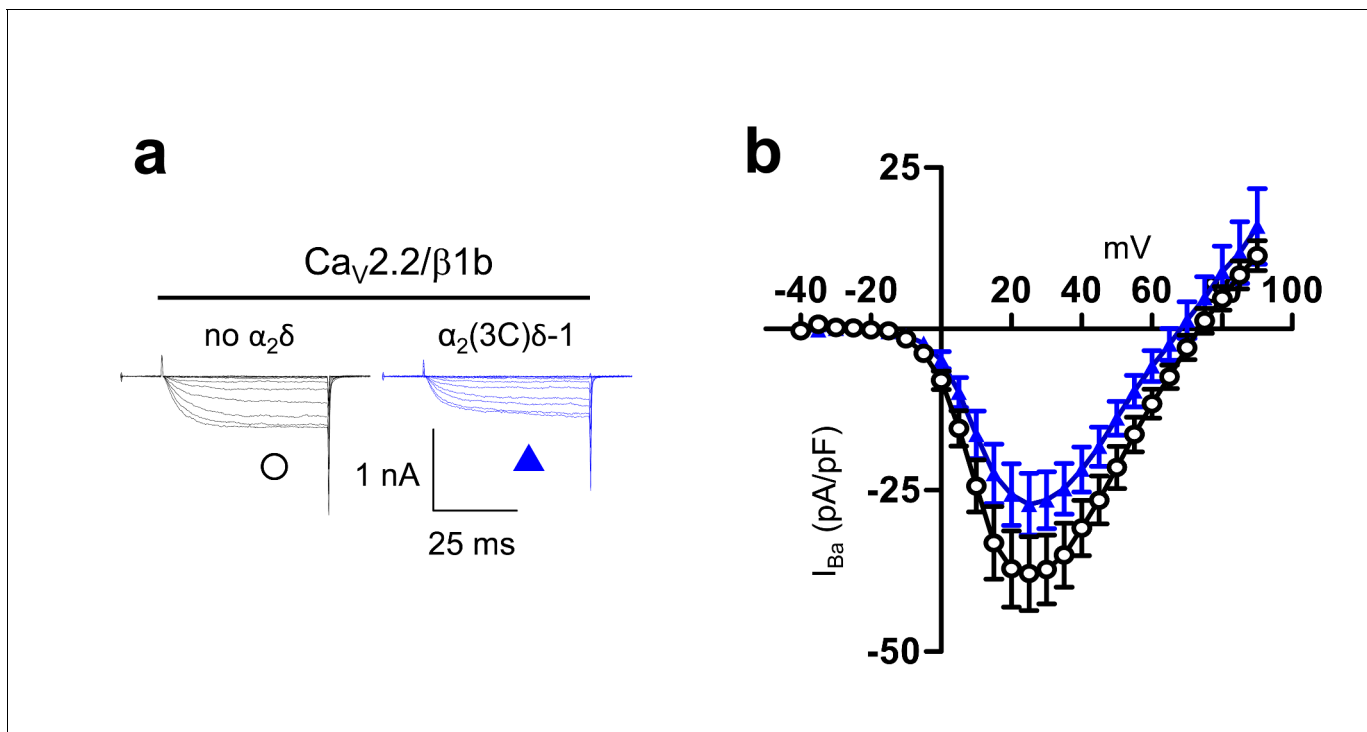DOI: 10.7554/eLife.21143.006

Figure 2—figure supplement 1. Examination of effect of $\alpha_2(3C)\delta$-1 on $Ca_V2.2/\beta1b$ calcium channel currents in tsA-201 cells. These experiments were performed using 10 mM Ba^{2+} to amplify any differences in current amplitude between the two conditions examined. (**a**) Example traces (-25 to $+25$ mV steps) for $Ca_V2.2/\beta1b$-GFP and either no $\alpha_2\delta$ (black traces) or $\alpha_2(3C)\delta$-1 (blue traces). The scale bars refer to all traces. (**b**) Mean ($\pm$ SEM) *IV* curves for experiments including those in (**a**), for $Ca_V2.2/\beta1b$-GFP and either no $\alpha_2\delta$ (black open circles, n = 10) or $\alpha_2(3C)\delta$-1-HA (blue triangles, n = 14). Peak I_{Ba} at +25 mV was -37.9 ± 5.7 pA/pF and -27.2 ± 4.8 pA/pF, respectively. G_{max} values were 0.91 ± 0.19 and 0.76 ± 0.12 nS/pF, respectively. $V_{50,act}$ values were 13.1 ± 1.6, and 14.9 ± 1.0 mV, respectively.
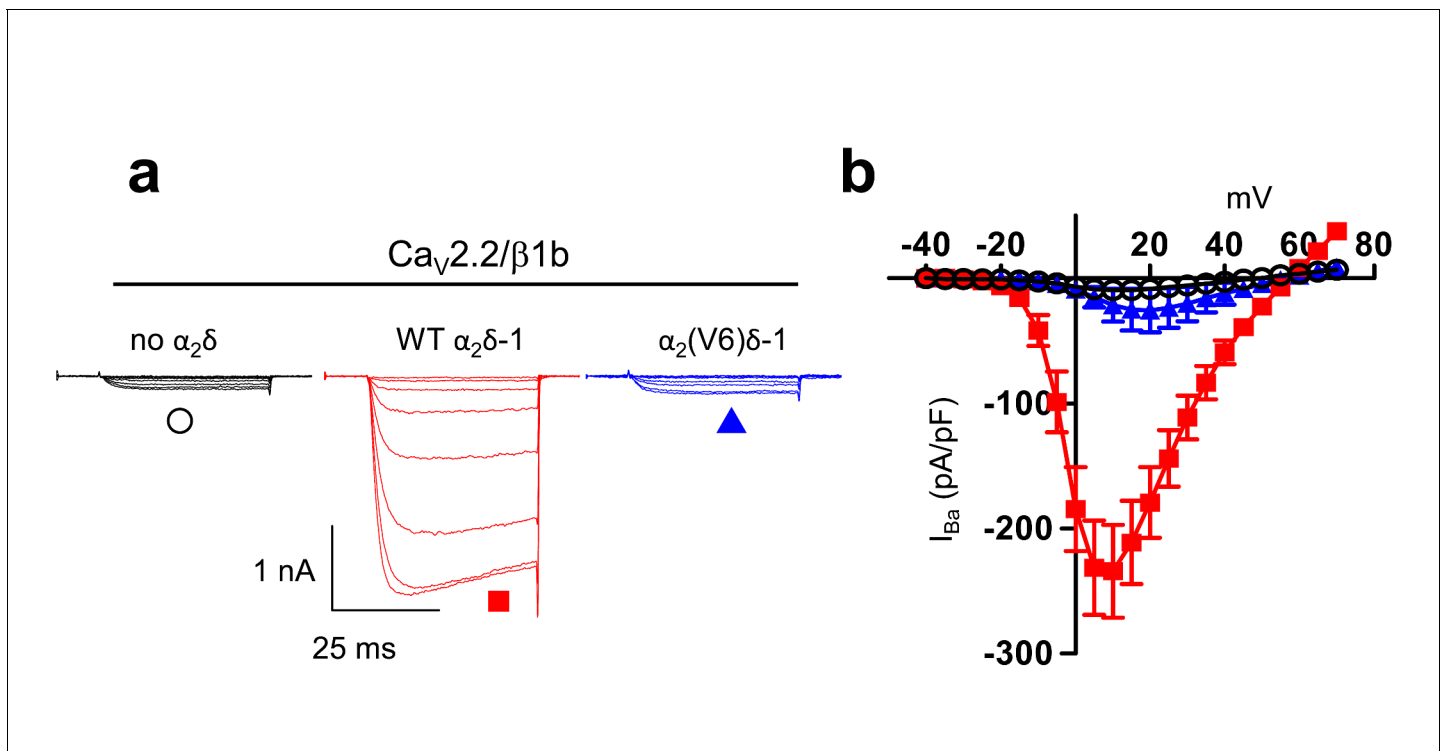
DOI: 10.7554/eLife.21143.007

Figure 2—figure supplement 2. Examination of effect of $\alpha_2(V6)\delta$-1 on $Ca_V2.2/\beta1b$ calcium channel currents in tsA-201 cells. (a) Example traces (-25 to $+10$ mV in 5 mV steps) for $Ca_V2.2/\beta1b$-GFP and either no $\alpha_2\delta$ (black traces), $\alpha_2\delta$-1 (red traces) or $\alpha_2(V6)\delta$-1 (blue traces). The scale bars refer to all traces. Charge carrier 1 mM Ba^{2+} (b) Mean (± SEM) *IV* curves for experiments including those in (c), for $Ca_V2.2/\beta1b$-GFP and either no $\alpha_2\delta$ (black open circles, n = 8), WT $\alpha_2\delta$-1 (red squares, n = 7) or $\alpha_2(V6)\delta$-1 (blue triangles, n = 8). G_{max} values were 0.32 ± 0.04, 6.72 ± 1.09 and 0.83 ± 0.52 nS/pF, respectively. $V_{50, act}$ values were 3.6 ± 2.2,,–0.7 ± 1.1 and 5.8 ± 1.1 mV, respectively.
DOI: 10.7554/eLife.21143.008

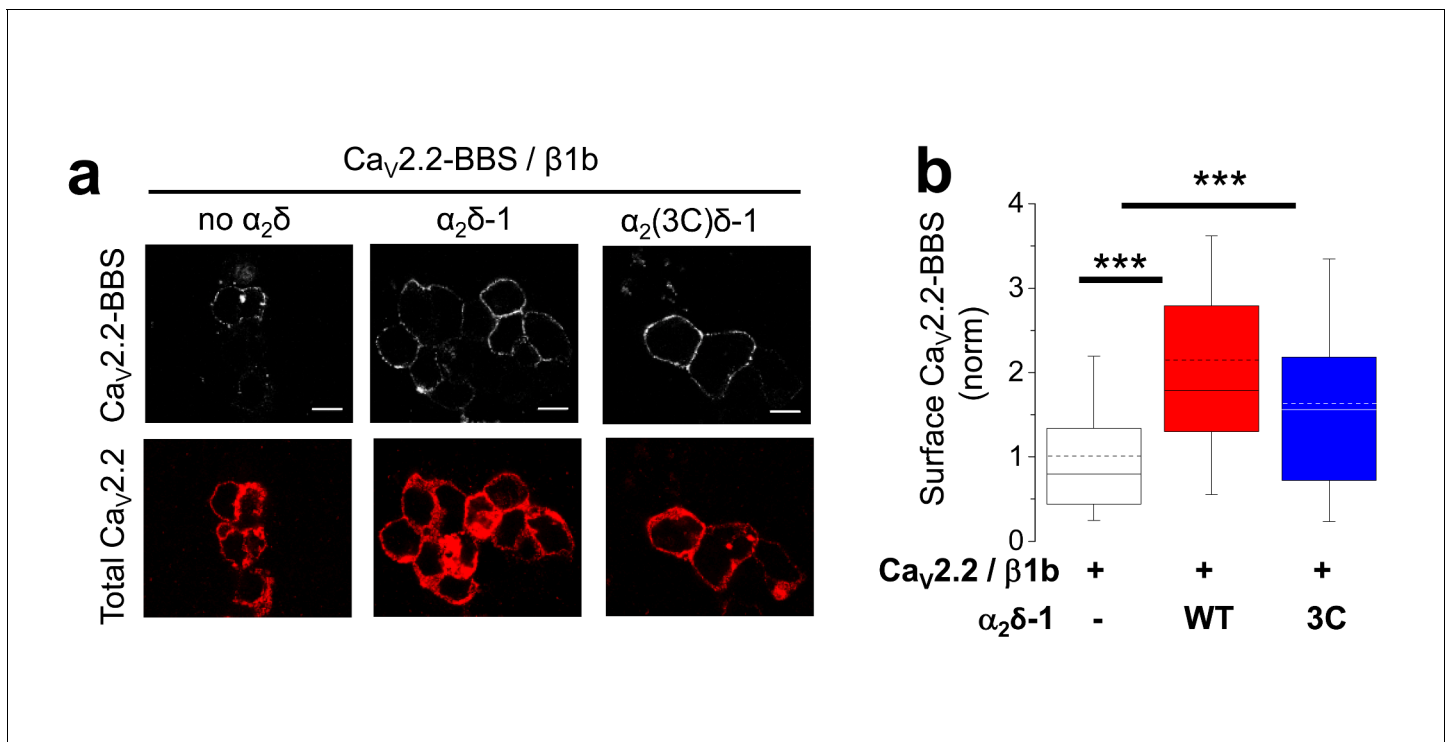**Figure 2—figure supplement 3.** Examination of effect of $\alpha_2(3C)\delta$-1 on Ca_V2.2/β1b cell surface expression in tsA-201 cells. (**a**) Immunocytochemical detection of cell-surface expression of Ca_V2.2-BBS, with β1b, and empty vector (left), WT $\alpha_2\delta$-1-HA (middle) or $\alpha_2(3C)\delta$-1-HA (right) in tsA-201 cells. Upper panel: Ca_V2.2-BBS cell-surface staining prior to permeabilization (grey-scale); lower panel: total Ca_V2.2 after permeabilization (II-III loop Ab, red). Scale bar 5 µm. (**b**) Quantification of Ca_V2.2-BBS cell-surface expression in tsA-201 cells (box and 10%–90% whisker plots) with empty vector (open bar, n = 191), WT $\alpha_2\delta$-1 (red bar, n = 175) or $\alpha_2(3C)\delta$-1 (blue bar, n = 177). N = 3 experiments. Statistical differences: ANOVA and Bonferroni post-hoc test; ***$p<0.001$, compared to no $\alpha_2\delta$.
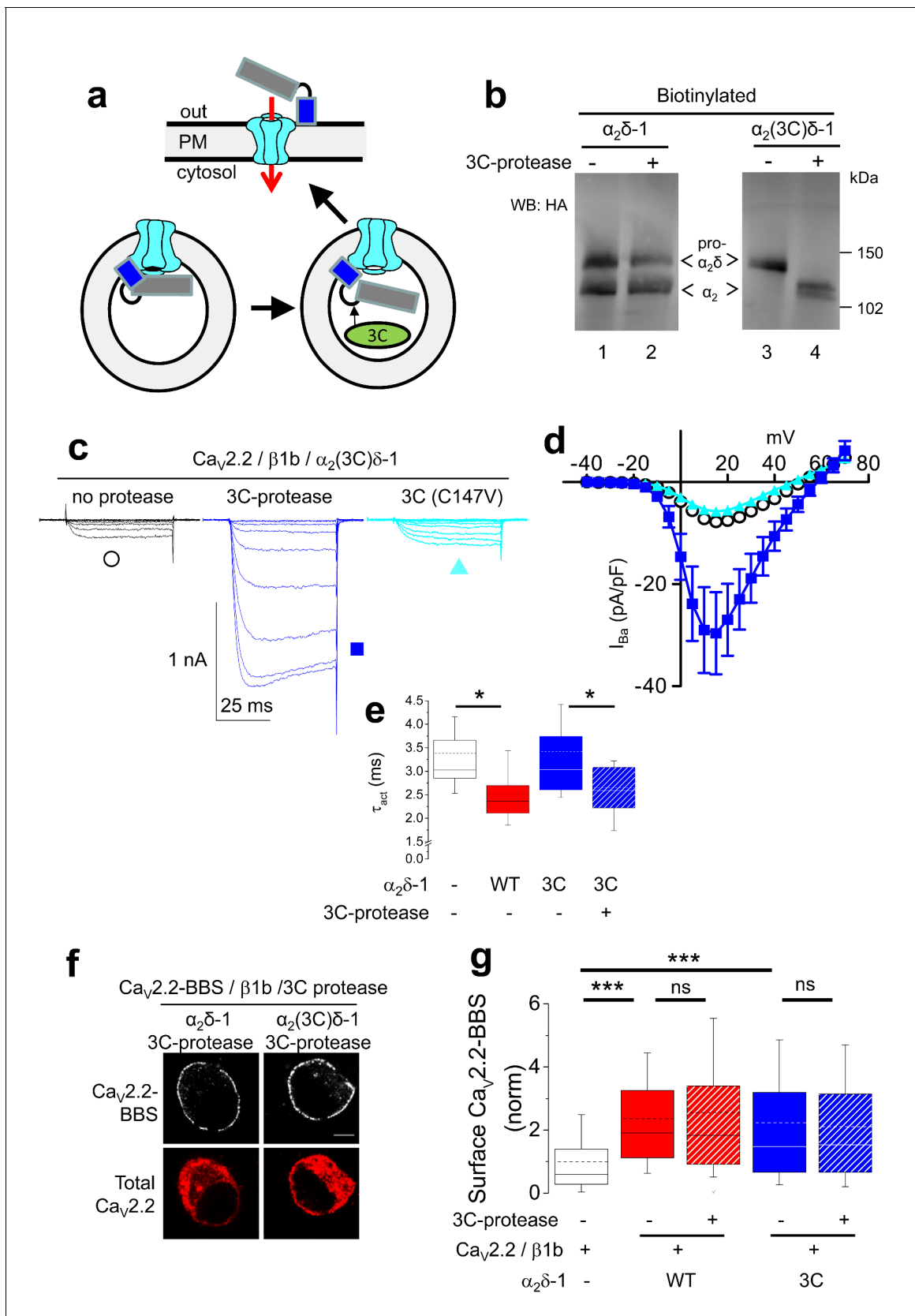DOI: 10.7554/eLife.21143.009

Figure 3. Effect of proteolytic cleavage of $\alpha_2\delta$-1 containing an HRV-3C cleavage site on cell-surface expression and functional properties of $Ca_V2.2$. (**a**) Cartoon showing intracellular cleavage by 3C-protease (green) of $\alpha_2(3C)\delta$-1 (gray/blue) associated with $Ca_V2.2$ (cyan). (**b**) Deglycosylated, cell-surface

Figure 3 continued on next page

Figure 3 continued

biotinylated fractions for $\alpha_2\delta$-1-HA (lanes 1 and 2) and α_2(3C)δ-1-HA (lanes 3 and 4), expressed in tsA-201 cells without (lanes 1 and 3) or with (lanes 2 and 4) 3C-protease. Representative of n = 4 experiments. WCL in *Figure 3—figure supplement 1* (c) Example traces (−30 to +10 mV steps) for Ca$_V$2.2/ β1b-GFP/α_2(3C)δ-1-HA and no protease (black traces), 3C-protease (blue traces) or inactive mutant 3C-(C147V) protease (cyan traces). Charge carrier 1 mM Ba^{2+}. Scale bars refer to all traces. (d) Mean (± SEM) *IV* curves for Ca$_V$2.2/β1b-GFP/α_2(3C)δ-1-HA and no protease (black open circles, n = 26), 3C-protease (blue squares, n = 22) or 3C-(C147V)-protease (cyan triangles, n = 23). G$_{max}$: 0.26 ± 0.04, 0.90 ± 0.22 and 0.22 ± 0.03 nS/pF, respectively. G$_{max}$ values in the presence of the active 3C-protease were greater than in the absence of protease or presence of 3C-(C147V)-protease (Kruskal-Wallis test with Dunn's multiple comparison post-hoc test, p<0.05). V$_{50,act}$: 6.05 ± 0.82, 5.18 ± 0.74 and 6.20 ± 1.20 mV, respectively. (e) Time constant of activation (τ_{act}) for I$_{Ba}$ at +10 mV for Ca$_V$2.2/β1b-GFP with no $\alpha_2\delta$-1 (open bar, n = 14), WT $\alpha_2\delta$-1-HA (red bar, n = 25), α_2(3C)δ-1-HA (blue bar, n = 21) or α_2(3C)δ-1-HA + 3C-protease (blue hatched bar, n = 17). Box and whisker plots. Statistical significance determined by ANOVA and Bonferroni's post-hoc test (*p<0.05). (f) Immunocytochemical detection of cell-surface Ca$_V$2.2-BBS, plus β1b, and $\alpha_2\delta$-1-HA (left panel) or α_2(3C)δ-1-HA (right panel), with 3C-protease. Upper panel: Ca$_V$2.2-BBS cell-surface staining (grey-scale), lower panel total Ca$_V$2.2 (II-III loop staining). Scale bar 5 μm. (g) Lack of effect of 3C-protease (hatched bars) on cell-surface expression of Ca$_V$2.2-BBS following expression of Ca$_V$2.2-BBS/β1b in N2A cells, with no $\alpha_2\delta$ (open bar, n = 206), WT $\alpha_2\delta$-1 (red bar, n = 212), WT $\alpha_2\delta$-1 and 3C-protease (red hatched bar, n = 192), α_2(3C)δ-1 (blue bar, n = 181) or α_2(3C)δ-1 and 3C-protease (blue hatched bar, n = 200). Box and whisker plots. Statistical differences determined by ANOVA and Bonferroni's post-hoc test (***p<0.001; ns: p>0.05).
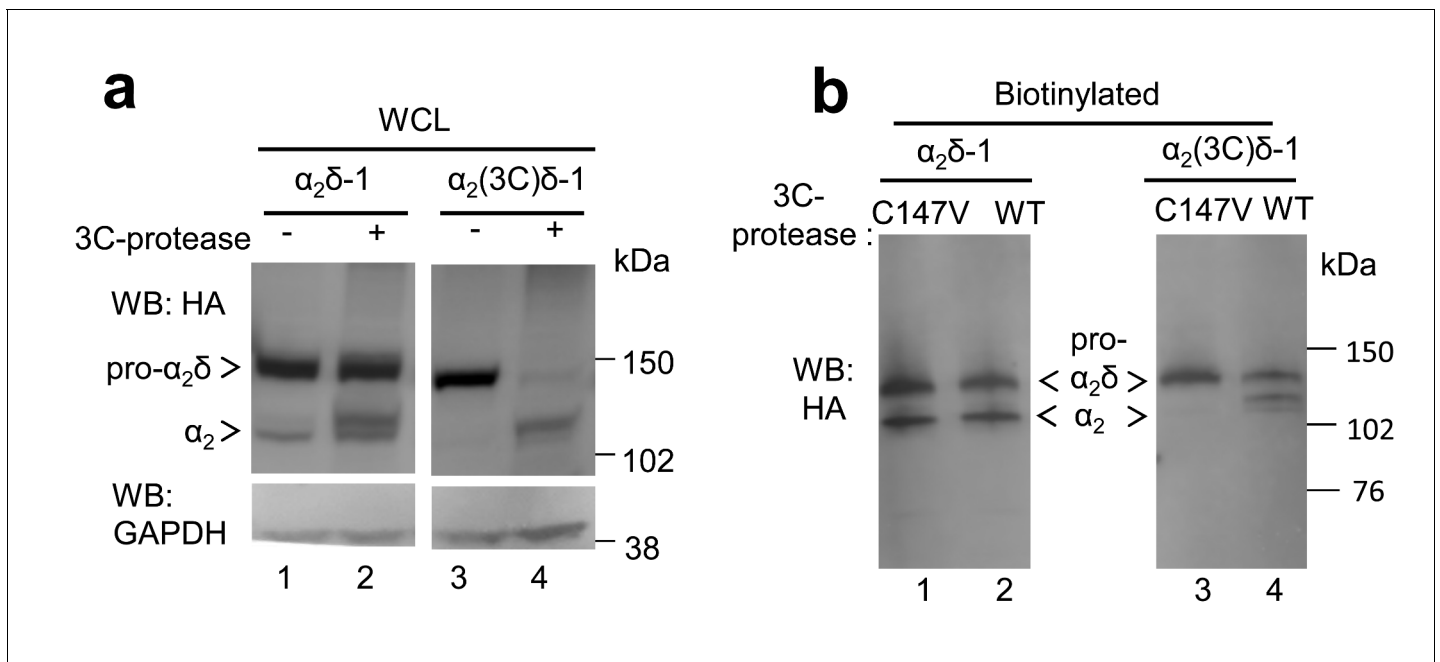
Figure 3—figure supplement 1. The effect of 3C-protease on $\alpha_2\delta$-1 and $\alpha_2(3C)\delta$-1 expressed in tsA-201 cells. (**a**) Deglycosylated WCL for the experiment shown in *Figure 3b*; $\alpha_2\delta$-1-HA (lanes 1 and 2) and $\alpha_2(3C)\delta$-1-HA (lanes 3 and 4), expressed in tsA-201 cells, without (lanes 1 and 3) or with (lanes 2 and 4) 3C-protease. Upper panel shows HA blot, lower panel: shows GAPDH blot loading control. (**b**) Cell surface biotinylation for $\alpha_2\delta$-1-HA (lanes 1 and 2) and $\alpha_2(3C)\delta$-1-HA (lanes 3 and 4), expressed in tsA-201 cells with inactive C147V (lanes 1 and 3) or (lanes 2 and 4) 3C-protease. Proteins were deglycosylated. WB was performed with HA Ab.
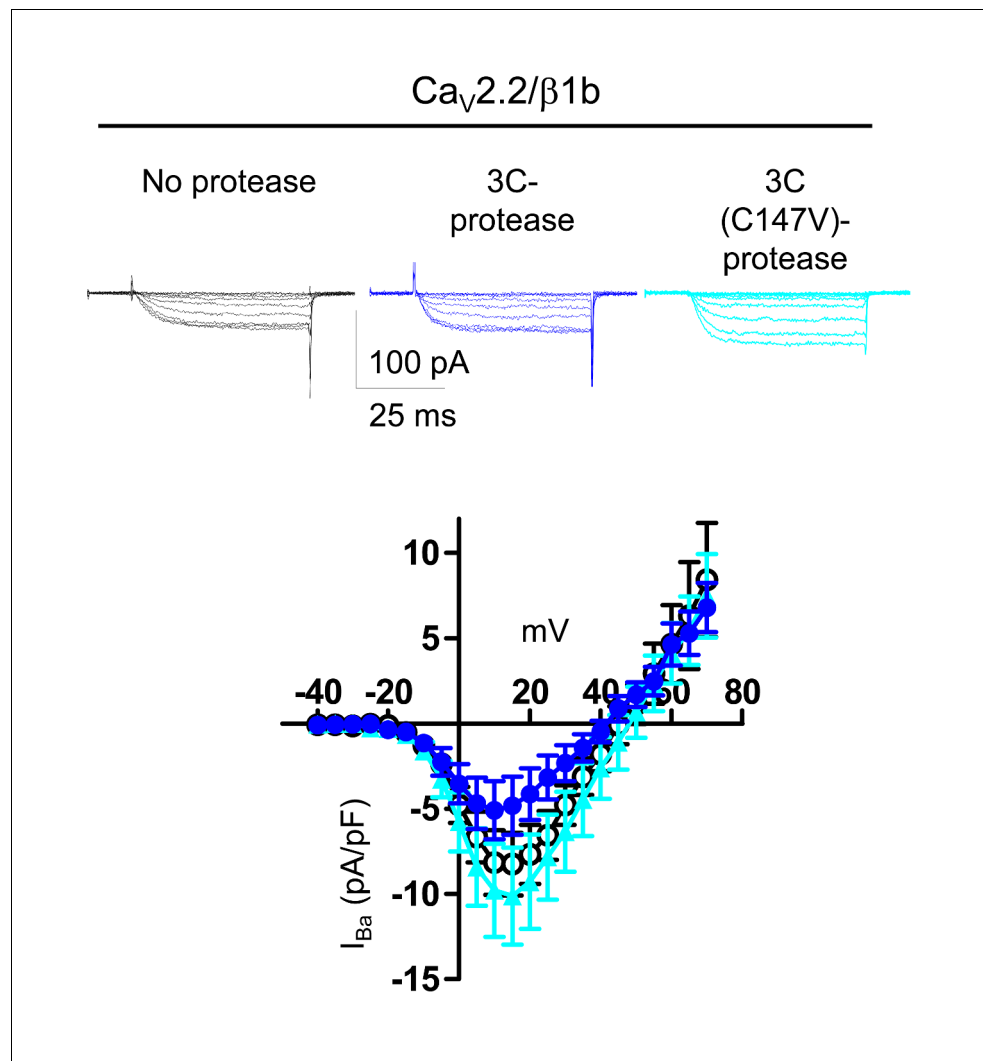DOI: 10.7554/eLife.21143.011

Figure 3—figure supplement 2. Lack of effect of 3C-protease on Ca$_V$2.2/β1b currents expressed in tsA-201 cells. Top: example traces (−25 to +15 mV steps) for Ca$_V$2.2/β1b-GFP and either no protease (black traces), WT 3C-protease (blue traces) or inactive mutant 3C-protease (C147V, cyan traces). The charge carrier was 1 mM Ba^{2+}. The scale bars refer to all traces. Bottom: Mean (± SEM) *IV* curves for experiments including those shown, for Ca$_V$2.2/β1b-GFP and either no protease (black open circles, n = 9), WT 3C-protease (blue circles, n = 11) or inactive mutant 3C-protease (C147V) (cyan triangles, n = 9). Peak I$_{Ba}$ at +15 mV was −8.2 ± 1.8 pA/pF, −4.8 ± 1.7 pA/pF and −10.1 ± 2.8 pA/pF, respectively. G$_{max}$ values were 0.32 ± 0.08, 0.20 ± 0.06 and 0.36 ± 0.09 nS/pF, respectively. V$_{50, act}$ values were 4.1 ± 0.7, 1.2 ± 1.2 and 3.8 ± 1.0 mV, respectively.
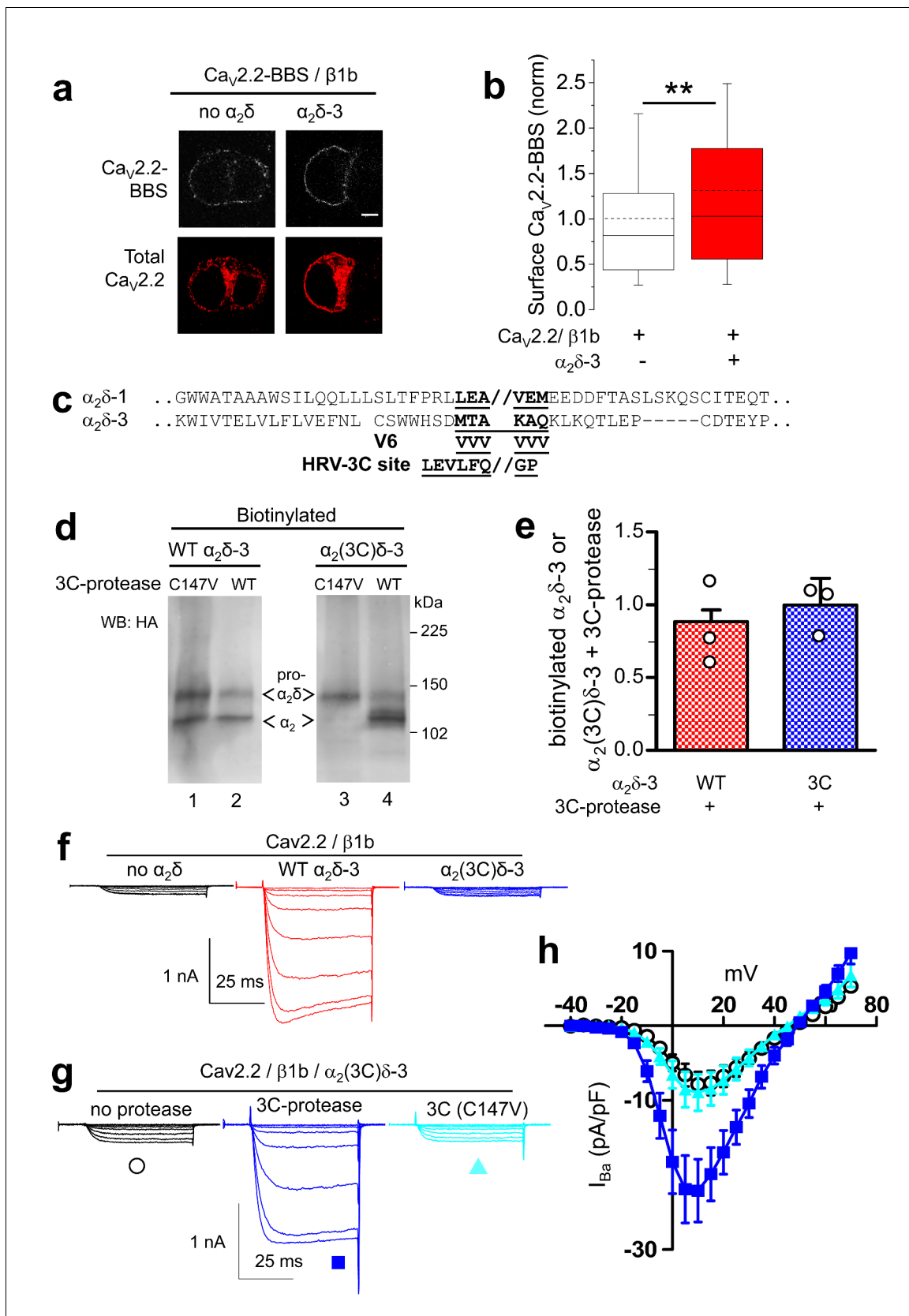DOI: 10.7554/eLife.21143.012

Figure 4. Effect of proteolytic cleavage of $\alpha_2\delta$-3 containing an HRV-3C cleavage site on cell-surface expression and functional properties of $Ca_V2.2$. (a) Images showing cell-surface $Ca_V2.2$-BBS (upper row, white), and total $Ca_V2.2$ (II-III loop Ab, lower row, red), for $Ca_V2.2$-BBS/β1b in N2A cells, with

Figure 4 continued on next page

Figure 4 continued

empty vector (panel 1) or $\alpha_2\delta$-3-HA (panel 2). Scale bar 5 µm. (**b**) Quantification (box and whisker plots) of effect $\alpha_2\delta$-3 on cell-surface Ca$_V$2.2-BBS following expression of Ca$_V$2.2-BBS/β1b with empty vector (open bar, n = 188) or WT $\alpha_2\delta$-3 (red bar, n = 188). Statistical difference determined by Student's t test, **p=0.0028. (**c**) Alignment of $\alpha_2\delta$-3 sequence around the predicted cleavage site with $\alpha_2\delta$-1, showing weak homology. Underlined sequence (MTAKAQ) mutated to V6 or HRV-3C cleavage motif. (**d**) $\alpha_2\delta$-3-HA (lanes 1, 2) and α_2(3C)δ-3-HA (lanes 3, 4) expressed in tsA-201 cells, with either inactive (C147V, lanes 1, 3) or WT 3C-protease (WT, lanes 2, 4), cell-surface biotinylated and deglycosylated. Full WB and corresponding WCL in *Figure 4—figure supplement 3* (**e**) Quantification of cell-surface expression of WT $\alpha_2\delta$-3-HA (red speckled bar) and α_2(3C)δ-3-HA (blue speckled bar), with 3C-protease, normalized relative to inactive 3C-protease (C147V) for n = 3 experiments. Data are mean (± SEM) and individual data points: p=0.4721 for WT $\alpha_2\delta$-3-HA and p=0.9513 for α_2(3C)δ-3 (1 sample t-test compared to respective control). (**f**) Example traces (−30 to +5 mV steps) for Ca$_V$2.2/β1b-GFP with no $\alpha_2\delta$ (black traces), WT $\alpha_2\delta$-3 (red traces) or α_2(3C)δ-3 (blue traces). G$_{max}$: 0.24 ± 0.03, 1.46 ± 0.22 and 0.21 ± 0.03 nS/pF respectively. V$_{50,act}$: 0.91 ± 1.015, 1.01 ± 0.85 and 4.03 ± 1.04 mV, respectively. (**g**) Example traces (−30 to +10 mV steps) for Ca$_V$2.2/β1b-GFP/α_2(3C)δ-3 and no protease (black traces), 3C-protease (blue traces) or inactive 3C-protease (C147V) (cyan traces). For (**f**) and (**g**), charge carrier 1 mM Ba^{2+}, scale bars refer to all traces. (**h**) Mean (± SEM) *IV* curves for Ca$_V$2.2/β1b-GFP/α_2(3C)δ-3 without protease (black open circles, n = 28), with 3C-protease (blue squares, n = 29) or inactive 3C-(C147V)-protease (cyan triangles, n = 24). G$_{max}$: 0.28 ± 0.05, 0.70 ± 0.11 and 0.30 ± 0.08 nS/pF, respectively. G$_{max}$ for 3C-protease condition larger than other two conditions (Kruskal-Wallis test with Dunn's post-hoc test, p<0.05). V$_{50, act}$: 4.0 ± 0.7, 0.3 ± 0.7 and 1.5 ± 0.6 mV, respectively.
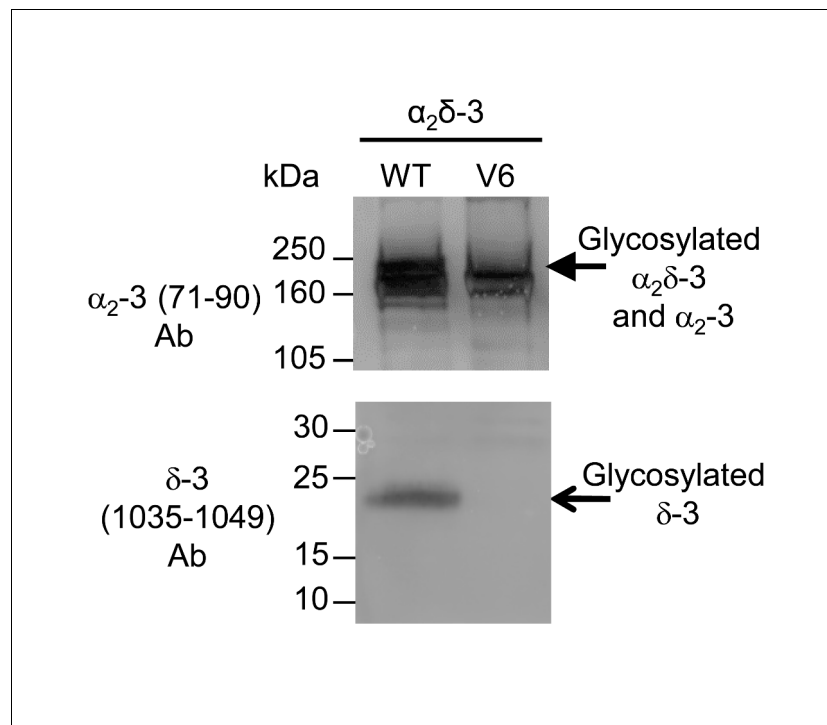
Figure 4—figure supplement 1. Lack of cleavage of α_2(V6)δ-3. The expression of $\alpha_2\delta$-3 compared to α_2(V6)δ-3. The constructs were expressed transiently in tsA-201 cells; peak lipid raft fractions were taken for western blotting. There was a complete loss of free δ-3 (lower panel) in α_2(V6)δ-3 (lane 2), compared to WT $\alpha_2\delta$-3 (lane 1). $\alpha_2\delta$-3 is shown in the upper panel.
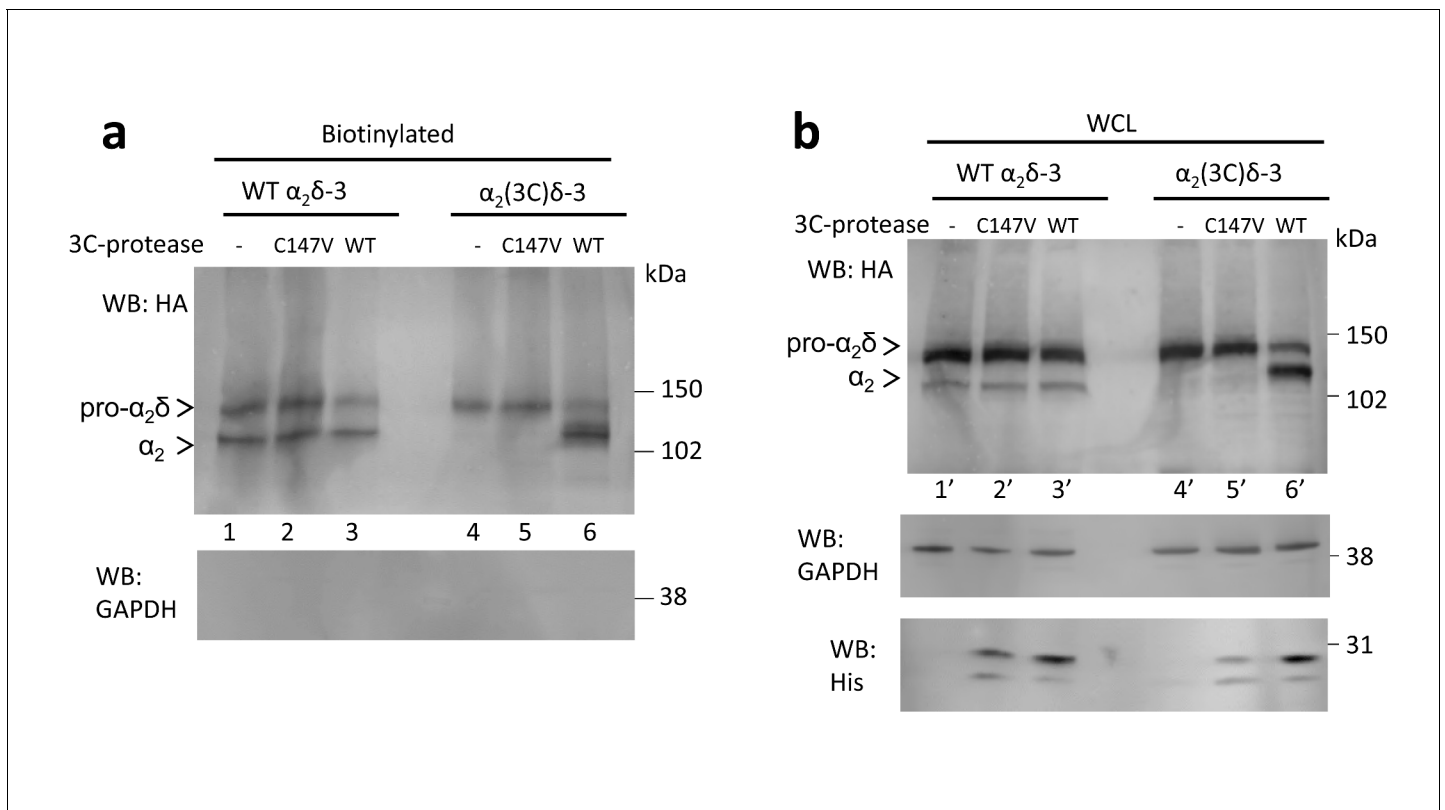
DOI: 10.7554/eLife.21143.014

Figure 4—figure supplement 2. Effect of 3C-protease on expression and cleavage of $\alpha_2(3C)\delta$-3. Full data from experiment shown in *Figure 4d*. WT $\alpha_2\delta$-3-HA (lanes 1, 2 and 3) and $\alpha_2(3C)\delta$-3-HA (lanes 4, 5 and 6) were expressed in tsA-201 cells, either without or with inactive (C147V, lanes 2 and 5) or WT 3C-protease (WT, lanes 3 and 6), subjected to cell surface biotinylation and streptavidin pull-down. Proteins were deglycosylated with PNGase-F. (a) shows biotinylated proteins and (b) shows WCL. The upper blot with HA Ab, shows that WT, but not inactive mutant, 3C-protease cleaved $\alpha_2(3C)\delta$-3 (lane 6). The lower blot shows GAPDH, indicating that no intracellular proteins were biotinylated, and the bottom blot in (b) shows expression of the His-tagged 3C-proteases.
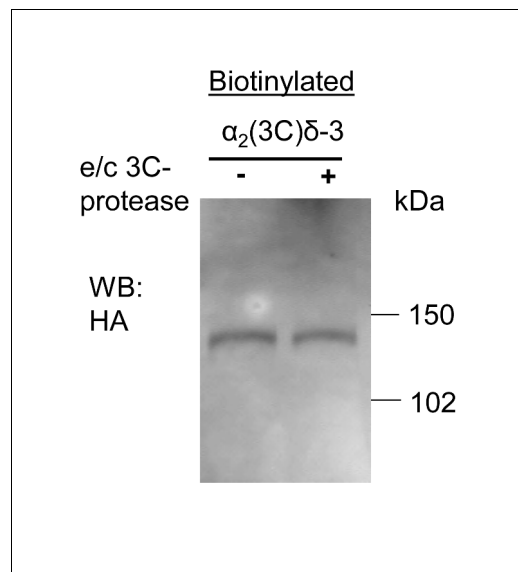DOI: 10.7554/eLife.21143.015

Figure 4—figure supplement 3. Lack of effect of purified 3C-protease on expression and cleavage of $\alpha_2(3C)\delta$-3. Incubation of cells expressing $\alpha_2(3C)\delta$-3-HA with 3C-protease enzyme did not result in cleavage on the cell surface. Cell surface biotinylated deglycosylated $\alpha_2(3C)\delta$-3-HA, from cells incubated without (left) or with (right) 3C-protease.
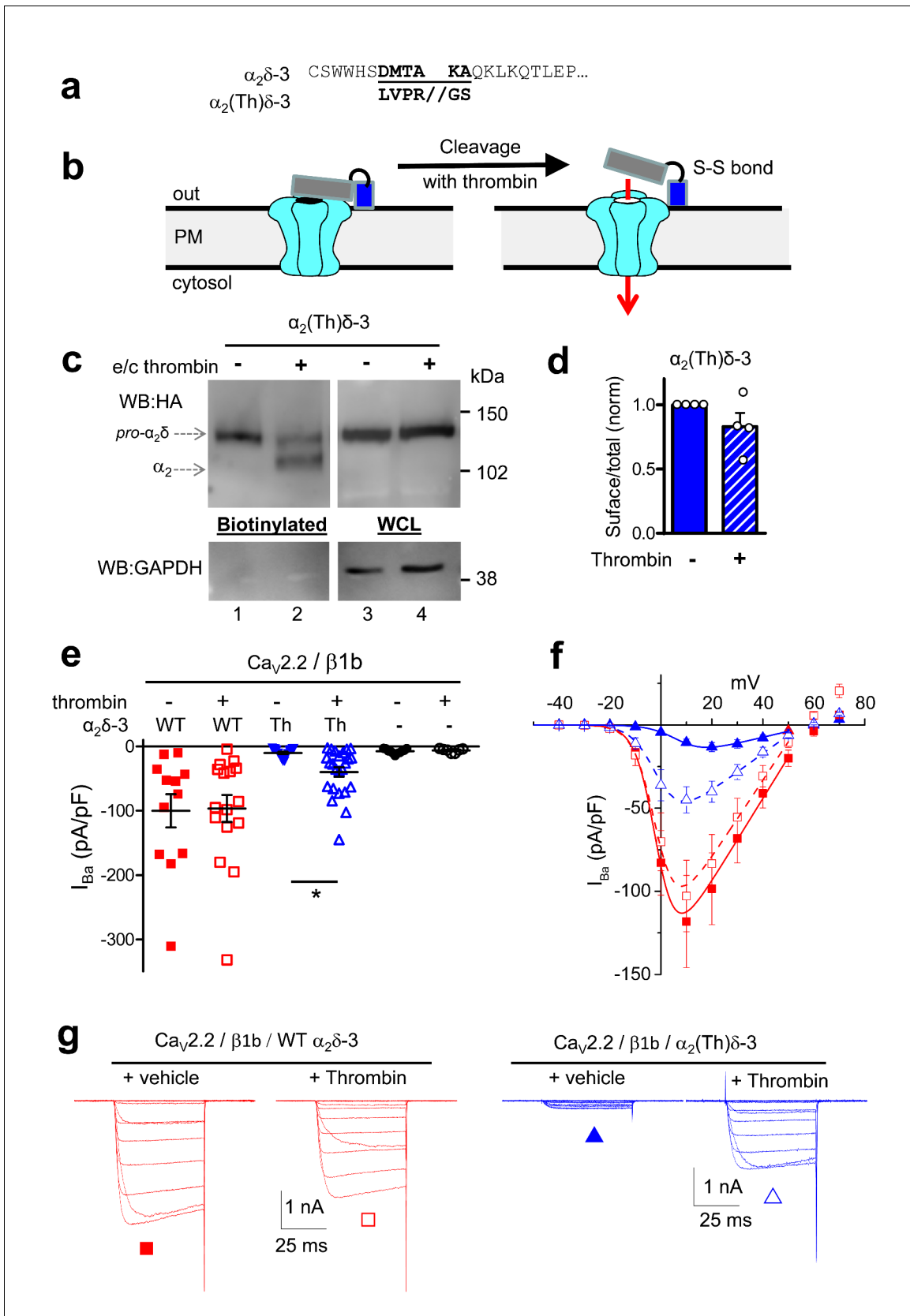DOI: 10.7554/eLife.21143.016

Figure 5. Effect of thrombin on the properties and function of $\alpha_2\delta$-3 containing a thrombin proteolytic cleavage site. (**a**) Sequence at $\alpha_2\delta$-3 cleavage site mutated to a thrombin cleavage site. (**b**) Cartoon of thrombin cleavage of $\alpha_2\delta$-3 on cell-surface. (**c**) Cell-surface biotinylation (left panel) shows

Figure 5 continued on next page

Figure 5 continued

efficient cleavage of cell-surface $\alpha_2(Th)\delta$-3-HA (lane 2), with no effect on total $\alpha_2(Th)\delta$-3-HA in WCL (right panel, lane 4). Samples were deglycosylated prior to loading. (**d**) Quantification of cell surface biotinylation experiments such as those shown in (**c**), indicating that thrombin does not decrease the amount of $\alpha_2(Th)\delta$-3-HA on the cell surface (hatched blue bar), normalized to vehicle application in each experiment (solid blue bar). Mean (± SEM) and individual data points for n = 4; p=0.2105, 1 sample t test. (**e**) Mean (± SEM) and individual data points of peak I_{Ba} at +10 mV, for $Ca_V2.2/\beta1b$ with WT $\alpha_2\delta$-3 (red squares), $\alpha_2(Th)\delta$-3 (blue triangles) or no $\alpha_2\delta$ (black circles) and either no protease (closed symbols), or 60 min thrombin incubation (open symbols). The charge carrier was 2 mM Ba^{2+}. For data without or with thrombin, respectively, n = 12, 16 for WT $\alpha_2\delta$-3; 15, 24 for $\alpha_2(Th)\delta$-3 and 11, 7 without $\alpha_2\delta$, from at least 3 independent transfections. Statistical difference between thrombin and vehicle determined by Kruskal-Wallis ANOVA and Dunn's multiple comparison post-hoc test, *p<0.05. (**f**) Mean (± SEM) full *IV* curves for the same conditions as in (**e**) (excluding the no $\alpha_2\delta$ data), fitted with a modified Boltzmann equation to +50 mV. G_{max} values (nS/pF) were 2.80 ± 0.61 (WT $\alpha_2\delta$-3; n = 10), 2.60 ± 0.55 (WT $\alpha_2\delta$-3 plus thrombin, n = 15), 0.43 ± 0.08 ($\alpha_2(Th)\delta$-3; n = 14), 1.26 ± 0.21 ($\alpha_2(Th)\delta$-3 plus thrombin, n = 21). $V_{50,act}$ values (mV) were +0.44 ± 1.71 (WT $\alpha_2\delta$-3), + 0.55 ± 1.28 (WT $\alpha_2\delta$-3 plus thrombin), +9.34 ± 0.08 ($\alpha_2(Th)\delta$-3), +0.87 ± 1.38 ($\alpha_2(Th)\delta$-3 plus thrombin). (**g**) Example Ba^{2+} currents (from −50 to +60 mV) for the four conditions shown in (**f**).

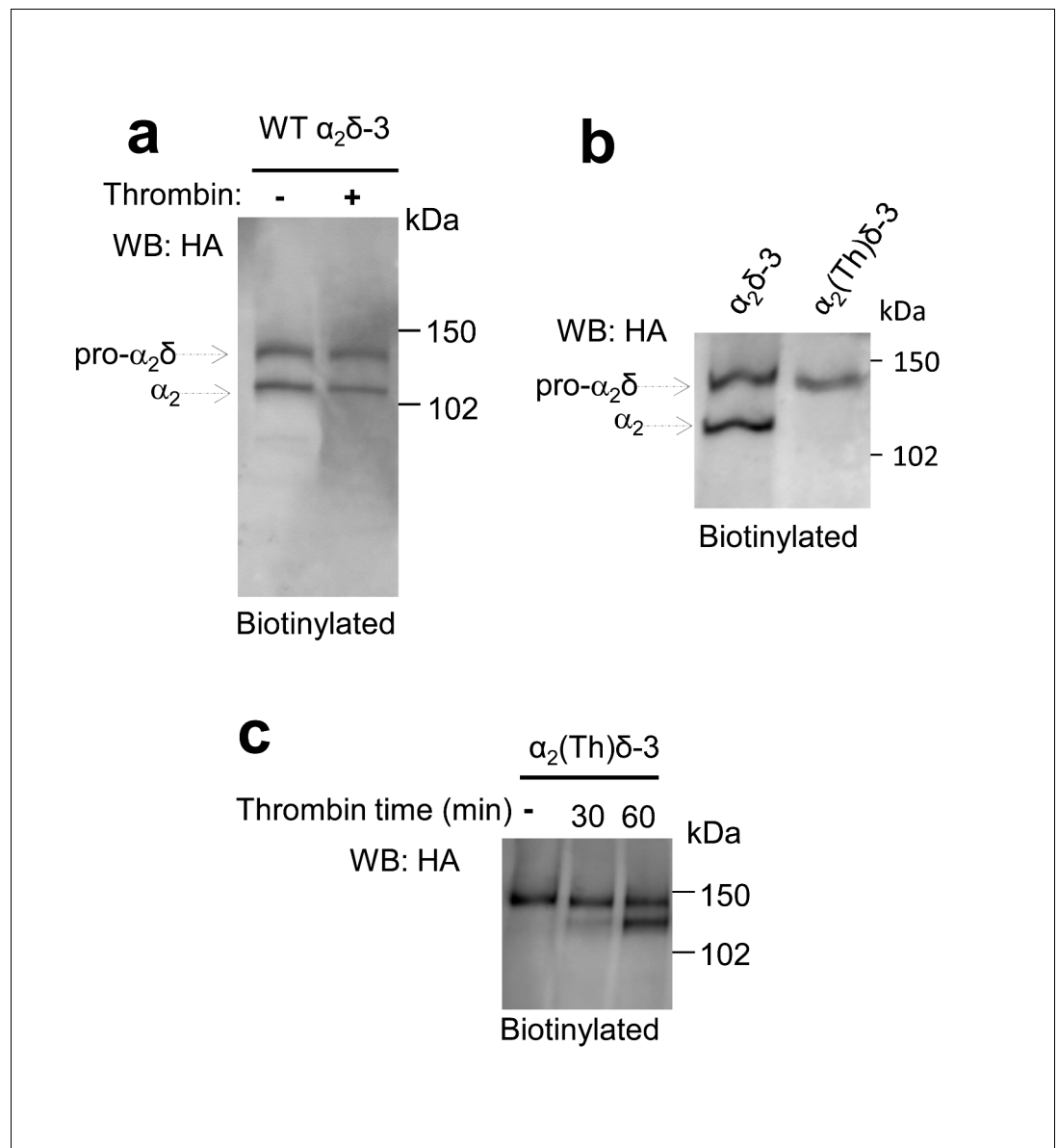**Figure 5—figure supplement 1.** Controls for cleavage of $\alpha_2(Th)\delta$-3 by thrombin. (**a**) Deglycosylated cell surface biotinylation for tsA-201 cells expressing WT $\alpha_2\delta$-3-HA and incubated either with vehicle or thrombin for 60 min (lanes 1 and 2), showing WT $\alpha_2\delta$-3 is not cleaved by thrombin. (**b**) Deglycosylated cell surface biotinylation for tsA-201 cells expressing WT $\alpha_2\delta$-3-HA or $\alpha_2(Th)\delta$-3-HA (lanes 1 and 2), showing $\alpha_2(Th)\delta$-3 reaches cell surface. (**c**) Deglycosylated cell surface biotinylation for tsA-201 cells expressing $\alpha_2(Th)\delta$-3-HA and incubated with thrombin for 0, 30 and 60 min (lanes 1–3), showing $\alpha_2(Th)\delta$-3 is cleaved on cell surface at 60 min.
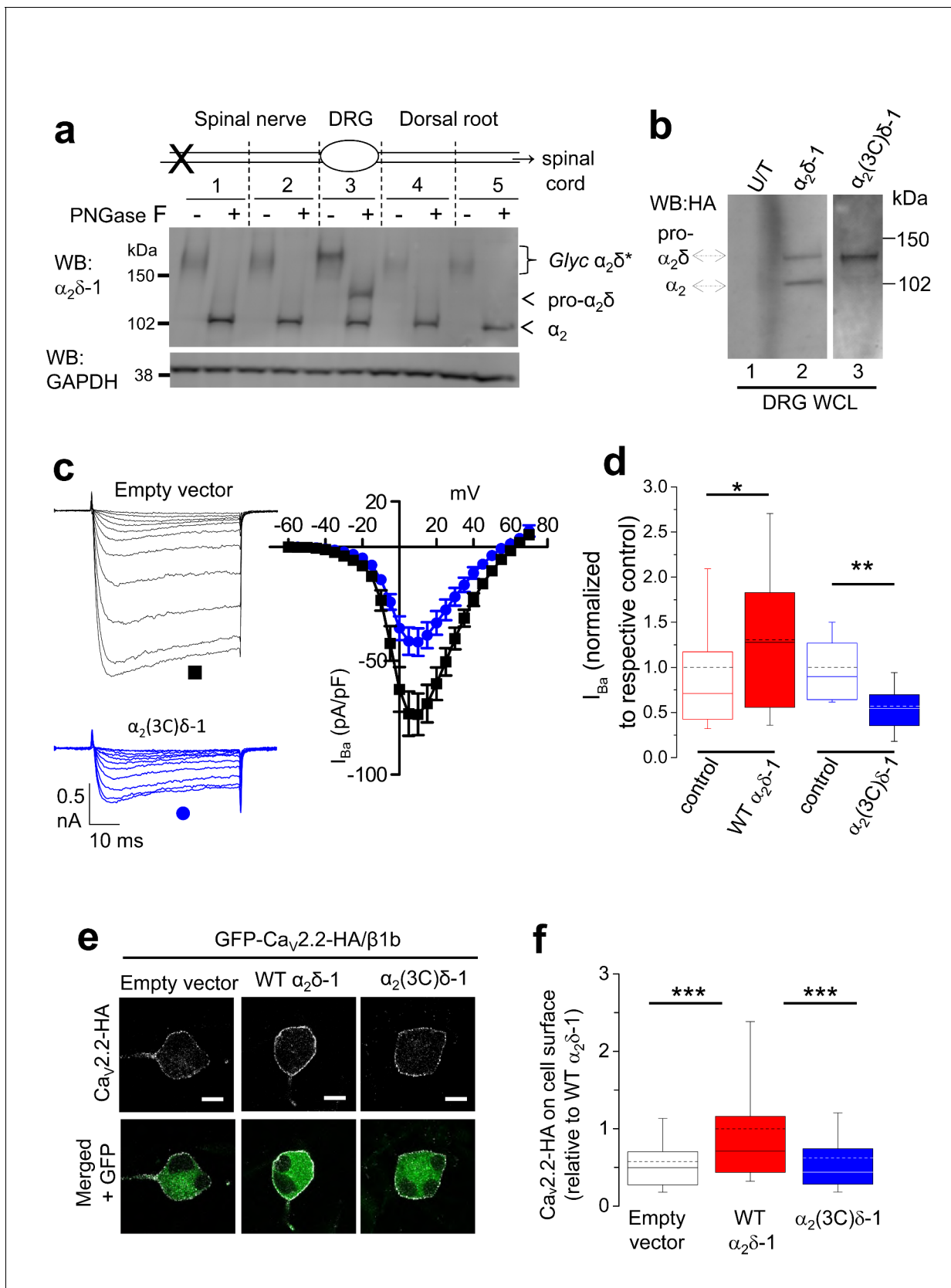DOI: 10.7554/eLife.21143.018

Figure 6. Proteolytic processing of endogenous $\alpha_2\delta$-1 and effect of exogenous expression of $\alpha_2\delta$-1 and $\alpha_2(3C)\delta$-1 in DRGs. (a) DRGs, spinal nerves and dorsal roots from rats, 4 days after SNL, were dissected and segmented according to the diagram. X marks site of ligation. Tissue was pooled from 4

Figure 6 continued on next page

Figure 6 continued

rats. It was either treated or not with PNGase-F as indicated, and reduced with DTT; deglycosylation allows resolution of two α_2-immunoreactive bands. Unprocessed $\alpha_2\delta$-1 is present only in the cell body compartment (segment 3) and is distinct from processed α_2-1 (indicated by arrows). Lower blot is GAPDH loading control. (b) WCL for empty vector-transfected DRGs (U/T, lane 1); WT $\alpha_2\delta$-1-HA-transfected DRGs (lane 2); α_2(3C)δ-1-HA transfected DRGs (lane 3). WB: anti-HA. (c) Left: Example traces (−45 to +5 mV steps) for control (empty vector-transfected) DRG neurons (black traces, top) and DRGs transfected with α_2(3C)δ-1 (blue traces, bottom). The charge carrier is 1 mM Ba^{2+}. The scale bars refer to all traces. Right: Mean (± SEM) *IV* curves for control DRG neurons (black squares, n = 12) and DRGs transfected with α_2(3C)δ-1 (blue circles, n = 14), from 3 independent experiments. G_{max} values were 2.20 ± 0.30 and 1.26 ± 0.14 nS/pF, respectively; p=0.0061 (Student's t test). $V_{50,\ act}$ values were −1.5 ± 1.2 and −1.5 ± 0.7 mV, respectively. (d) Comparison of normalized peak I_{Ba} in control DRGs (open red bar, n = 55) and WT $\alpha_2\delta$-1-transfected DRGs (closed red bar, n = 54) including data from *Figure 2d* in, or comparison of control DRGs (open blue bar, n = 12) with α_2(3C)δ-1 transfected DRGs (closed blue bar, n = 14). Box and whisker plots. Statistical differences, Student's t test: *, p=0.048, **p=0.0067 compared to respective control. (e) Confocal optical sections (1 μm) showing GFP-$Ca_V2.2$-HA in non-permeabilized DRG neurons (top, white), when co-transfected with β1b and either empty vector (left), WT $\alpha_2\delta$-1 (middle) or α_2(3C)δ-1 (right). GFP fluorescence is shown in the merged lower panel. Scale bars: 10 μm. (f) Box and whisker plot of cell surface HA fluorescence density as a ratio of internal GFP density for $Ca_V2.2$-HA expression in DRG somata, transfected with empty vector (open bar, n = 81), WT $\alpha_2\delta$-1 (red bar, n = 133) or α_2(3C)δ-1 (blue bar, n = 159). ***p<0.001, 1 way ANOVA and Bonferroni post hoc test.
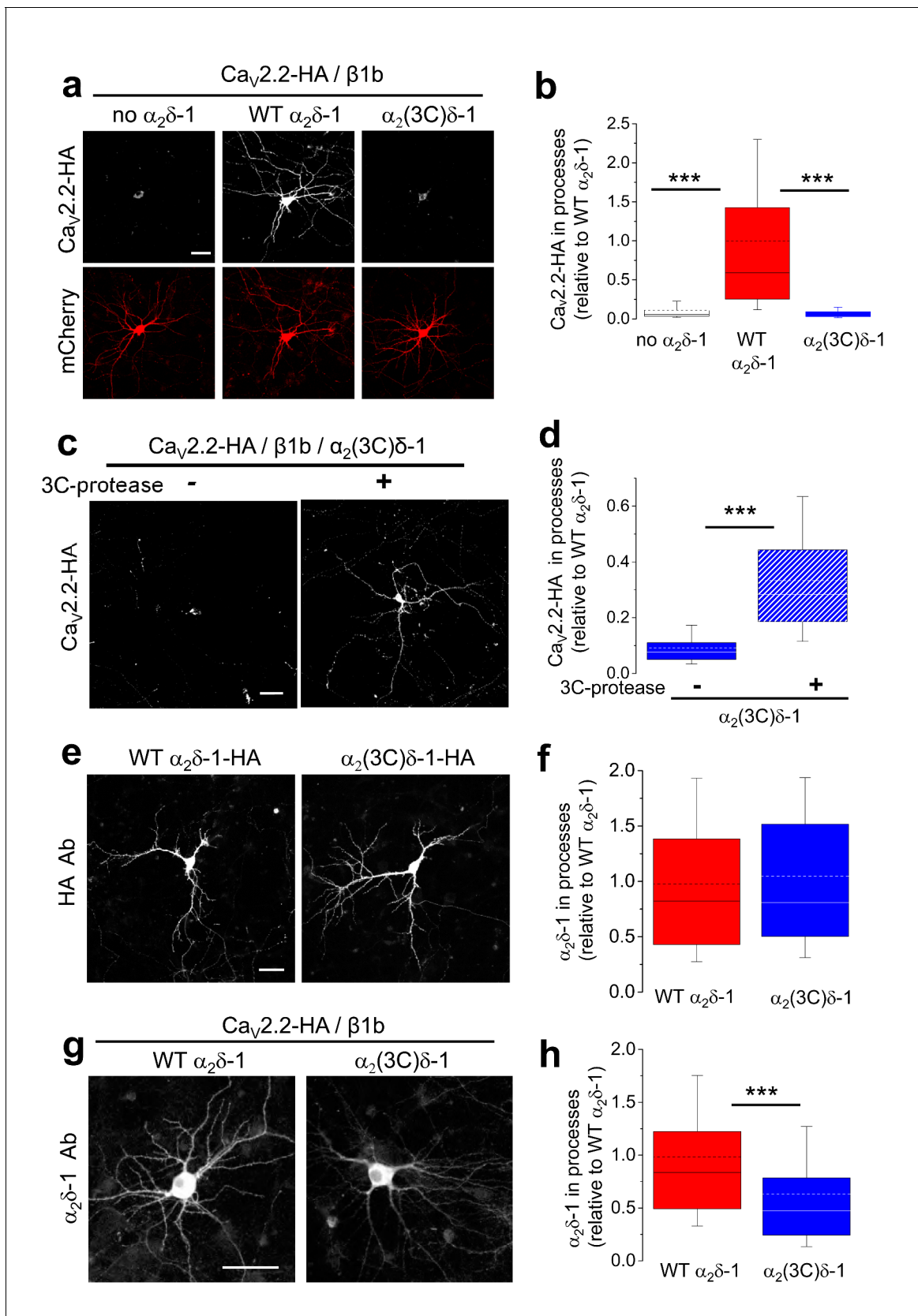
DOI: 10.7554/eLife.21143.019

Figure 7. Effect of $\alpha_2\delta$-1 and proteolytic cleavage of α_2(3C)δ-1 on trafficking of Ca$_V$2.2 into hippocampal neurites. (a) Images showing Ca$_V$2.2-HA in permeabilized hippocampal neurons (top, white), when co-transfected with β1b, mCherry (bottom, red) and either no $\alpha_2\delta$ (left), WT $\alpha_2\delta$-1 (middle) or

Figure 7 continued on next page

Figure 7 continued

$\alpha_2(3C)\delta$-1 (right). Scale bar: 50 μm applies to all images. (**b**) Box and whisker plots for Ca$_V$2.2-HA expression in processes without $\alpha_2\delta$ (open bar, n = 136 processes from 29 cells), with $\alpha_2\delta$-1 (red bar, n = 147 processes from 27 cells) or with $\alpha_2(3C)\delta$-1 (blue bar, n = 109 processes from 22 cells). ***p<0.001, 1 way ANOVA and Bonferroni *post hoc* test. (**c**) Images showing Ca$_V$2.2-HA in permeabilized hippocampal neurons (white), when co-transfected with β1b, $\alpha_2(3C)\delta$-1 and mCherry (transfection marker, not shown), either without (left) or with (right) 3C-protease. Scale bar: 50 μm applies to both images. (**d**) Box and whisker plots for Ca$_V$2.2-HA expression in processes with $\alpha_2(3C)\delta$-1, transfected without (solid blue bar, n = 191 processes), or with 3C-protease (blue hatched bar, n = 187 processes). ***p<0.001, 1 way ANOVA and Bonferroni *post hoc* test. (**e**) Images showing WT $\alpha_2\delta$-1-HA (left) or $\alpha_2(3C)\delta$-1-HA (right) expressed in permeabilized hippocampal neurons (white), co-transfected only with mCherry (transfection marker, not shown). Antigen retrieval was used prior to the HA Ab. Scale bar: 50 μm applies to both images. (**f**) Box and whisker plots for expression in the processes of WT $\alpha_2\delta$-1-HA (red bar, n = 248 processes from 52 cells) and $\alpha_2(3C)\delta$-1 (blue bar, n = 263 processes from 51 cells). (**g**) Images showing $\alpha_2\delta$-1 in hippocampal neurons (white), when transfected with Ca$_V$2.2-HA, β1b, mCherry (transfection marker, not shown) and either WT $\alpha_2\delta$-1 (left) or $\alpha_2(3C)\delta$-1 (right). Antigen retrieval was used prior to the $\alpha_2\delta$-1 mAb. Scale bar: 50 μm applies to both images. (**h**) Box and whisker plots for $\alpha_2\delta$-1 expression in hippocampal processes, for WT $\alpha_2\delta$-1 (red bar, n = 221 processes) and $\alpha_2(3C)\delta$-1 (blue bar, n = 184 processes). ***p<0.0001, Student's t test.
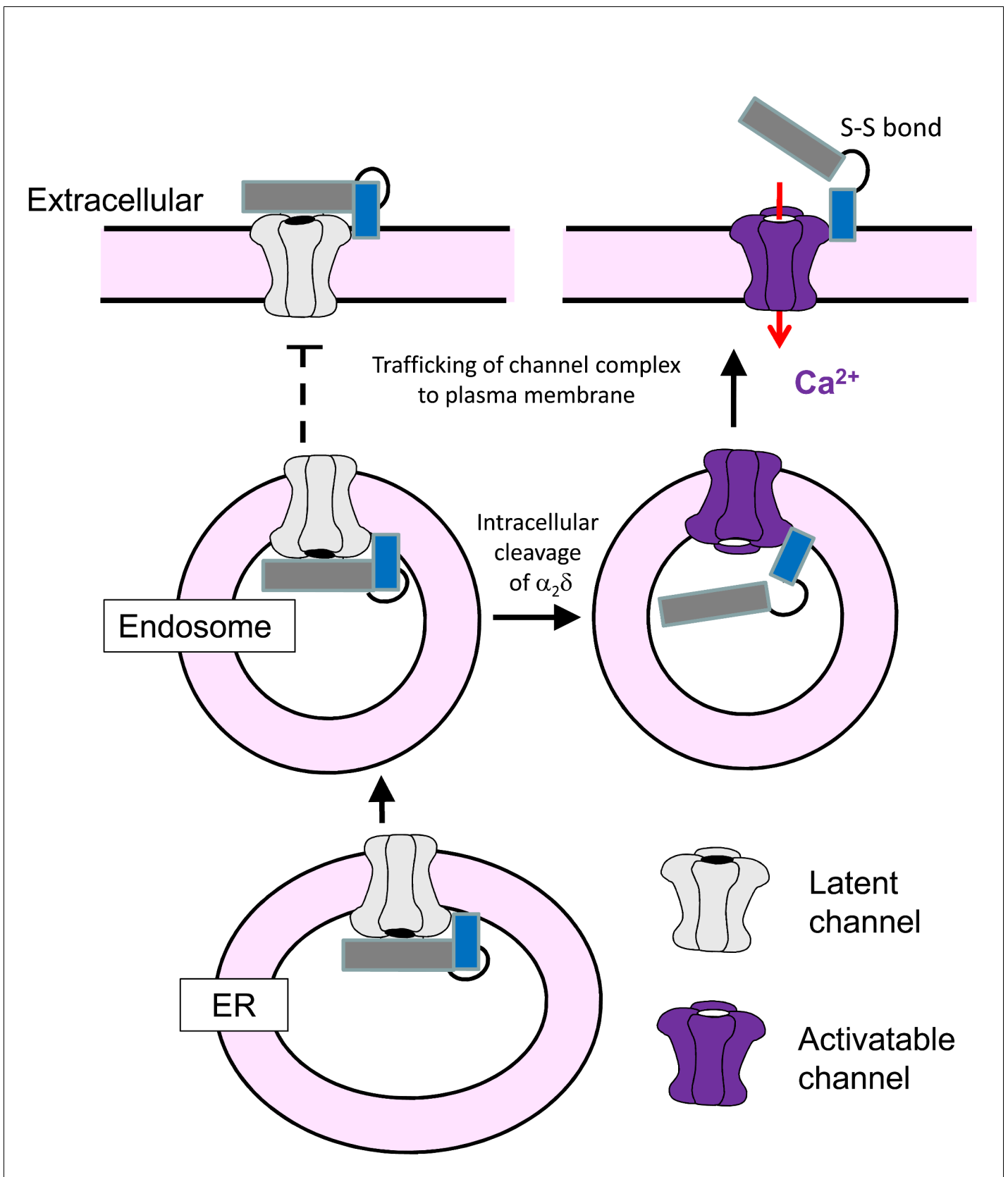
DOI: 10.7554/eLife.21143.020

Figure 7—figure supplement 1. Cartoon showing processing and trafficking of $\alpha_2\delta$ in neurons. Cartoon of the effect of proteolytic processing of $\alpha_2\delta$ (dark gray α_2, blue δ) on Ca$_V$2.2 trafficking and voltage-dependent activation. The gray channel is one that cannot be activated by depolarization, *Figure 7—figure supplement 1 continued on next page*

Figure 7—figure supplement 1 continued

whereas the purple channel is functional. The solid arrows indicate the likely trafficking pathway in neurons. The dotted lines show that trafficking of channels containing uncleaved $\alpha_2\delta$ to the plasma membrane and into processes, and extracellular proteolytic cleavage of $\alpha_2\delta$ indicates do not occur in native neurons studied here, although it is possible that this may occur in pathological conditions, for example following $\alpha_2\delta$-1 upregulation as a result of neuropathic nerve injury in DRG neurons.
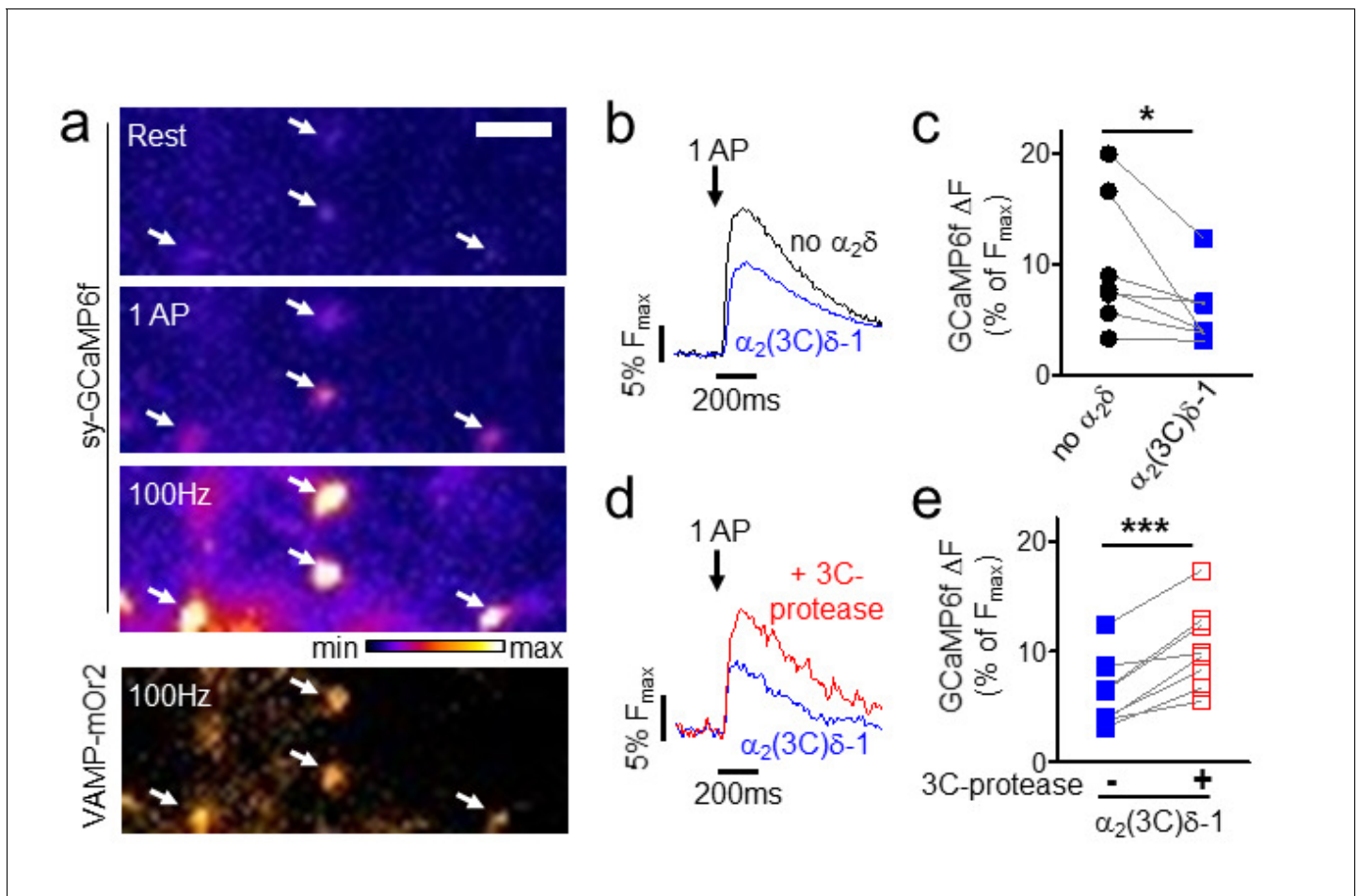
Figure 8. Effect of proteolytic cleavage of $\alpha_2(3C)\delta$-1 on Ca^{2+} influx in presynaptic terminals of hippocampal neurons. (**a**) Fluorescence changes in presynaptic terminals of hippocampal neurons expressing sy-GCaMP6f and VAMP-mOr2 in response to electrical stimulation. White arrows point to transfected boutons. Top three panels show sy-GCaMP6f fluorescence: at rest (top), after 1 AP (middle) and after 100 Hz stimulation for 1 s (bottom). The bottom panel shows VAMP-mOr2 fluorescence after 100 Hz stimulation for 1 s. Scale bar 5 µm. The pseudocolour scale is shown below the third panel. (**b**) Mean example traces from the same experiment of sy-GCaMP6f fluorescence changes in response to 5 single APs from individual presynaptic terminals of neurons co-transfected with either empty vector (black trace) or $\alpha_2(3C)\delta$-1 (blue trace). (**c**) Sy-GCaMP6f fluorescence changes (expressed as % of F_{max}) in response to 1 AP from boutons co-transfected with either empty vector (black filled circles) or $\alpha_2(3C)\delta$-1 (blue filled squares) (n = 7 independent experiments, *p=0.049, paired t test). (**d**) Mean example traces of sy-GCaMP6f fluorescence changes in response to 5 single APs from presynaptic terminal of neurons co-transfected with either $\alpha_2(3C)\delta$-1 (blue trace) or $\alpha_2(3C)\delta-1$ + 3C-protease (red trace). (**e**) Sy-GCaMP6f fluorescence changes (expressed as % of F_{max}) in response to 1 AP from boutons co-transfected with either $\alpha_2(3C)\delta$-1 (blue filled squares) or $\alpha_2(3C)\delta-1$ + 3C-protease (red open squares) (n = 8 independent experiments, ***p=0.0005, paired t test).
DOI: 10.7554/eLife.21143.022